151-0660-00L: Model Predictive Control **(Due: 16/05/19)**

Programming Exercise

Instructor: Melanie Zeilinger *Names:* Mayank Mittal, Ossama Ahmed, Marta Tintore Gazulla

Let $T_i^c(t)$ denote the temperature of the zone i at time $t \geq 0$, and $p_i^c(t)$ be the cooling power of unit i. The outside temperature is given by T_o. The system parameters for each zone i are defined as follows:

- m_i: thermal mass
- w_i: external heat flux
- $\alpha_{i,j}$: thermal conductivity between zone i and zone j

Given modelling equations of the system dynamics:

$$
\begin{aligned}
m_1\dot{T}_1^c(t) &= \alpha_{1,2}(T_2^c(t) - T_1^c(t)) + \alpha_{1,o}(T_o - T_1^c(t)) + p_1^c(t) + w_1 \\
m_2\dot{T}_2^c(t) &= \alpha_{1,2}(T_1^c(t) - T_2^c(t)) + \alpha_{2,3}(T_3^c(t) - T_2^c(t)) + \alpha_{2,o}(T_o - T_2^c(t)) + p_2^c(t) + w_2 \\
m_3\dot{T}_3^c(t) &= \alpha_{2,3}(T_2^c(t) - T_3^c(t)) + \alpha_{3,o}(T_o - T_3^c(t)) + w_3
\end{aligned}
$$

with the initial condition: $\mathbf{T_{init}} = [T_1^c(0), T_2^c(0), T_3^c(0)]^T$.

Solution 1: State Space Modelling *(2 pts.)*

Let $\mathbf{X^c}(t) = [T_1^c(t), T_2^c(t), T_3^c(t)]^T$ and $\mathbf{p^c}(t) = [p_1^c(t), p_2^c(t)]^T$, then $\mathbf{X^c}(0) = \mathbf{T_{init}}$. Re-writing the above system of equations in state space form:

$$
\begin{pmatrix} \dot{T}_1^c(t) \\ \dot{T}_2^c(t) \\ \dot{T}_3^c(t) \end{pmatrix} = \begin{pmatrix} \frac{-(\alpha_{1,o}+\alpha_{1,2})}{m_1} & \frac{\alpha_{1,2}}{m_1} & 0 \\ \frac{\alpha_{1,2}}{m_2} & \frac{-(\alpha_{2,o}+\alpha_{1,2}+\alpha_{2,3})}{m_2} & \frac{\alpha_{2,3}}{m_2} \\ 0 & \frac{\alpha_{2,3}}{m_3} & \frac{-(\alpha_{3,o}+\alpha_{2,3})}{m_3} \end{pmatrix} \begin{pmatrix} T_1^c(t) \\ T_2^c(t) \\ T_3^c(t) \end{pmatrix} + \begin{pmatrix} \frac{1}{m_1} & 0 \\ 0 & \frac{1}{m_2} \\ 0 & 0 \end{pmatrix} \begin{pmatrix} p_1^c(t) \\ p_2^c(t) \end{pmatrix}
$$

$$
+ \begin{pmatrix} \frac{1}{m_1} & 0 & 0 \\ 0 & \frac{1}{m_2} & 0 \\ 0 & 0 & \frac{1}{m_3} \end{pmatrix} \begin{pmatrix} \alpha_{1,o}T_o + w_1 \\ \alpha_{2,o}T_o + w_2 \\ \alpha_{3,o}T_o + w_3 \end{pmatrix},
$$

we get: $\dot{\mathbf{X}}^\mathbf{c}(t) = A^c\mathbf{X^c}(t) + B^c\mathbf{p^c}(t) + B_d^c\mathbf{d^c}$, where:

$$
A^c = \begin{pmatrix} \frac{-(\alpha_{1,o}+\alpha_{1,2})}{m_1} & \frac{\alpha_{1,2}}{m_1} & 0 \\ \frac{\alpha_{1,2}}{m_2} & \frac{-(\alpha_{2,o}+\alpha_{1,2}+\alpha_{2,3})}{m_2} & \frac{\alpha_{2,3}}{m_2} \\ 0 & \frac{\alpha_{2,3}}{m_3} & \frac{-(\alpha_{3,o}+\alpha_{2,3})}{m_3} \end{pmatrix} = 10^{-3} \begin{pmatrix} -0.4250 & 0.3750 & 0 \\ 0.1875 & -0.9375 & 0.5000 \\ 0 & 0.4000 & -1.0000 \end{pmatrix},
$$

$$
B^c = \begin{pmatrix} \frac{1}{m_1} & 0 \\ 0 & \frac{1}{m_2} \\ 0 & 0 \end{pmatrix} = 10^{-5} \begin{pmatrix} 0.5000 & 0 \\ 0 & 0.2500 \\ 0 & 0 \end{pmatrix},
$$

$$
B_d^c = \begin{pmatrix} \frac{1}{m_1} & 0 & 0 \\ 0 & \frac{1}{m_2} & 0 \\ 0 & 0 & \frac{1}{m_3} \end{pmatrix} = 10^{-5} \begin{pmatrix} 0.5000 & 0 & 0 \\ 0 & 0.2500 & 0 \\ 0 & 0 & 0.2000 \end{pmatrix},
$$

$$
\mathbf{d^c} = \begin{pmatrix} \alpha_{1,o}T_o + w_1 \\ \alpha_{2,o}T_o + w_2 \\ \alpha_{3,o}T_o + w_3 \end{pmatrix} = \begin{pmatrix} 100 \\ 1000 \\ 3000 \end{pmatrix}.
$$

Solution 2: Discretization of the System *(3 pts.)*

Given sampling time $T_s = 60$ units. We need to assume piece-wise constant input signals within the sampling intervals, i.e. $\mathbf{p^c}(kT_s + \tau) = \text{constant}, \forall \tau \in [0, T_s)$. Further, the disturbance $\mathbf{d^c} = \mathbf{d}$, where $\mathbf{d} = [d_1, d_2, d_3]^T$ is a constant.

For a linear time invariant system: $\dot{\mathbf{X}}^\mathbf{c}(t) = A^c\mathbf{X^c}(t) + B^c\mathbf{p^c}(t) + B_d^c\mathbf{d^c}$, we can write its solution as:

$$\mathbf{X^c}(t) = e^{A(t-t_0)}\mathbf{X^c}(t_0) + \int_{t_0}^{t} e^{A(t-\tau)}B\mathbf{p^c}(\tau)d\tau + (t-t_0)B_d^c\mathbf{d^c}$$

Let us denote $\mathbf{X}(k) = \mathbf{X^c}(kT_s)$. Then, by setting $t_0 = kT_s$ and $t = (k+1)T_s$, we can write:

$$\mathbf{X}(k+1) = e^{AT_s}\mathbf{X}(k) + \int_{kT_s}^{(k+1)T_s} e^{A((k+1)T_s-\tau)}B\mathbf{p^c}(\tau)d\tau + T_sB_d^c\mathbf{d}$$

Since we assume zero order hold over the input action i.e. $\mathbf{p}(k) = \mathbf{p^c}(kT_s + \tau) = \text{constant}, \forall \tau \in [0, T_s)$, we can simplify further:

$$\begin{aligned}
&\mathbf{X}(k+1) = e^{AT_s}\mathbf{X}(k) + \left(\int_{kT_s}^{(k+1)T_s} e^{A((k+1)T_s-\tau)}Bd\tau\right)\mathbf{p}(k) + T_sB_d^c\mathbf{d} \\
\implies &\mathbf{X}(k+1) = \underbrace{e^{AT_s}}_{A}\mathbf{X}(k) + \underbrace{\left(\int_0^{T_s} e^{A(\tau)}Bd\tau\right)}_{B}\mathbf{p}(k) + \underbrace{T_sB_d^c}_{B_d}\mathbf{d} \\
\implies &\mathbf{X}(k+1) = A\mathbf{X}(k) + B\mathbf{p}(k) + B_d\mathbf{d}
\end{aligned}$$

We calculate the state space model for the discretized plant using `MATLAB` in-built functions. For the sampling time $T_s = 60$ units, we get the following:

$$\begin{aligned}
A &= \begin{pmatrix} 0.9748 & 0.0216 & 0.003 \\ 0.0108 & 0.9458 & 0.0283 \\ 0.001 & 0.0226 & 0.9421 \end{pmatrix}, \\
B &= 10^{-3}\begin{pmatrix} 0.2962 & 0.0016 \\ 0.0016 & 0.1459 \\ 0 & 0.0017 \end{pmatrix}, \\
B_d &= 10^{-3}\begin{pmatrix} 0.3000 & 0 & 0 \\ 0 & 0.1500 & 0 \\ 0 & 0 & 0.1200 \end{pmatrix}.
\end{aligned}$$

Solution 3: Steady-State Formulation of the System *(2 pts.)*

Given desired temperatures: $T_{1,des} = -20^o$C and $T_{2,des} = 0.25^o$C. Zone 3 can be have any temperature. This implies that the reference tracking signal would be: $\mathbf{r} = [T_{1,des}, T_{2,des}]^T$.

Suppose at steady state, the temperature of the zones and applied inputs are given by $\mathbf{X}_{sp}$, and $\mathbf{p}_{sp}$ respectively. Since system is observable, i.e. $\mathbf{Y}(k) = \mathbf{X}(k)$, at steady state $\mathbf{r} = H\mathbf{X}_{sp}$ where $H = \begin{pmatrix} 1 & 0 & 0 \\ 0 & 1 & 0 \end{pmatrix}$.

$$
\begin{aligned}
&\implies \mathbf{X}_{sp} = A\mathbf{X}_{sp} + B\mathbf{p}_{sp} + B_d\mathbf{d}, \\
&\quad\ H\mathbf{X}_{sp} = \mathbf{r} \\
&\implies (\mathbb{I} - A)\mathbf{X}_{sp} - B\mathbf{p}_{sp} = B_d\mathbf{d}, \\
&\quad\ H\mathbf{X}_{sp} = \mathbf{r} \\
&\implies \begin{pmatrix} \mathbb{I} - A & B \\ H & 0 \end{pmatrix} \begin{pmatrix} \mathbf{X}_{sp} \\ \mathbf{p}_{sp} \end{pmatrix} = \begin{pmatrix} B_d\mathbf{d} \\ \mathbf{r} \end{pmatrix}
\end{aligned}
$$

By solving the above equation, we get: $\mathbf{X}_{sp} = [-20.00, 0.25, 6.25]^T$ and $\mathbf{p}_{sp} = [-1814.4, -647.2]^T$.

Let us assume: $\Delta\mathbf{p}(k) = \mathbf{p}(k) - \mathbf{p}_{sp}$, and $\Delta\mathbf{X}(k) = \mathbf{X}(k) - \mathbf{X}_{sp}$.

$$
\begin{aligned}
&\implies \mathbf{X}(k+1) = A\mathbf{X}(k) + B\mathbf{p}(k) + B_d\mathbf{d} \\
&\implies \mathbf{X}(k+1) - \mathbf{X}_{sp} = A(\mathbf{X}(k) - \mathbf{X}_{sp}) + B(\mathbf{p}(k) - \mathbf{p}_{sp}) \\
&\implies \Delta\mathbf{X}(k+1) = A\Delta\mathbf{X}(k) + B\Delta\mathbf{p}(k)
\end{aligned}
$$

Solution 4: Constraints on the System *(2 pts.)*

From the task description, different zones have the following constraints on the temperature (in ^{o}C):

$$
\begin{pmatrix} -\infty \\ 0 \\ -\infty \end{pmatrix} \leq \begin{pmatrix} T_1(k) \\ T_2(k) \\ T_3(k) \end{pmatrix} \leq \begin{pmatrix} -10 \\ 5 \\ \infty \end{pmatrix}.
$$

Further, the cooling units have the following limitations over the power supplied (in W):

$$
\begin{pmatrix} -2500 \\ -2000 \end{pmatrix} \leq \begin{pmatrix} p_1(k) \\ p_2(k) \end{pmatrix} \leq \begin{pmatrix} 0 \\ 0 \end{pmatrix}.
$$

Under the delta-formulation of the problem:

$$
\begin{pmatrix} -\infty \\ -0.25 \\ -\infty \end{pmatrix} \leq \Delta\mathbf{X}(k) \leq \begin{pmatrix} 10 \\ 4.75 \\ \infty \end{pmatrix}, \text{ and}
$$

$$
\begin{pmatrix} -685.6 \\ -1358.2 \end{pmatrix} \leq \Delta\mathbf{p}(k) \leq \begin{pmatrix} 1814.4 \\ 647.2 \end{pmatrix}.
$$

Solution 5: LQR Controller: Closed Loop Simulation for $T_0^{(1)}$ *(4 pts.)*

While designing the Q and R matrices, we keep them diagonal to separately penalize the states and inputs for each of the three zones.

For matrix Q, since there is no restriction on the temperature of zone 3, we do not need to penalize it. Further, the desired temperature for zone 1 is lower than that for zone 2. Thus, the penalization should be more for the former than for the latter.

For designing the R matrix, we keep the entries small since we want an aggressive controller to drive the system to the steady state quickly. That means, having small values in R enables inputs u to be bigger (therefore, ensures faster dynamics). The values are then fine-tuned to ensure that the constraints are not violated.

Using hit-and-trial motivated by the above intuitions, the following choices for the matrices Q and R were made:

$$Q = \begin{pmatrix} 3000 & 0 & 0 \\ 0 & 2000 & 0 \\ 0 & 0 & 0 \end{pmatrix}, \; R = \begin{pmatrix} 0.05 & 0 \\ 0 & 0.05 \end{pmatrix}$$

The plot in Figure 1 shows the closed-loop simulation obtained by using unconstrained optimal control law (LQR) with initial conditions: $T_0^{(1)} = T_{sp} + [3, 1, 0]^T$.

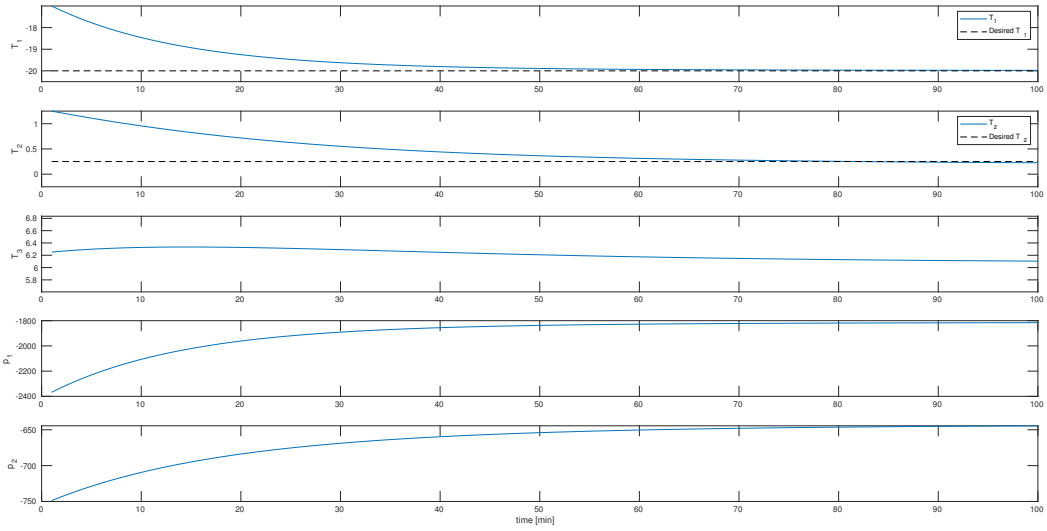

Figure 1: Closed-loop simulation of scenario 1 by following an LQR Control Law with initial setting $T_0^{(1)}$

Solution 6: LQR Controller: Infinite Horizon Cost *(1 pts.)*

For an LQR controller, we know:

$$\begin{aligned} J_\infty(\mathbf{X}(0)) &= \sum_{k=0}^{\infty} \mathbf{X}(k)^T Q \mathbf{X}(k) + \mathbf{u}(k)^T R \mathbf{u}(k) \\ &= \mathbf{X}(0)^T P_\infty \mathbf{X}(0) \end{aligned}$$

Using the above choices of Q and R and initial condition $T_0^{(1)}$, the infinite horizon cost at $t = 0$ for LQR control law is: 336526.22 units.

Solution 7: LQR Controller: Closed Loop Simulation for $T_0^{(2)}$ *(2 pts.)*

The plot in Figure 2 shows the closed-loop simulation obtained by using unconstrained optimal control law (LQR) with initial conditions: $T_0^{(2)} = T_{sp} + [-1, -0.1, -4.5]^T$.

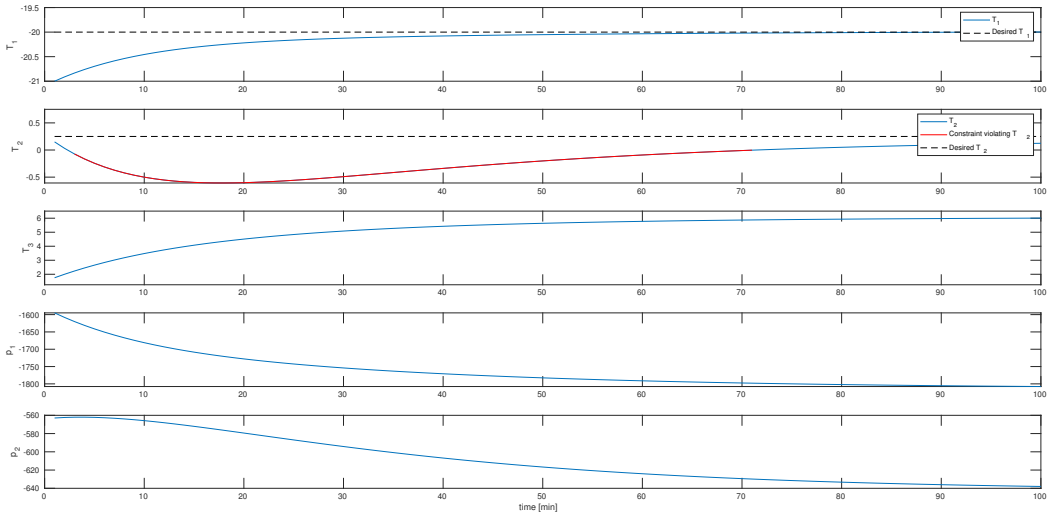

Figure 2: Closed-loop simulation of scenario 1 by following an LQR Control Law with initial setting $T_0^{(2)}$

Although the LQR control law makes the system converge to the desired equilibrium point T_{sp}, the temperature constraints of zone 2, T_2, is violated for the duration $t = 3$ units to $t = 71$ units. Such kind of violation is expected from the LQR controller as it does not take any constraints over the states and inputs into account.

Solution 8: LQR Controller: Invariant Set *(3 pts.)*

The invariant set obtained by following a LQR control law is shown in Figure 3.

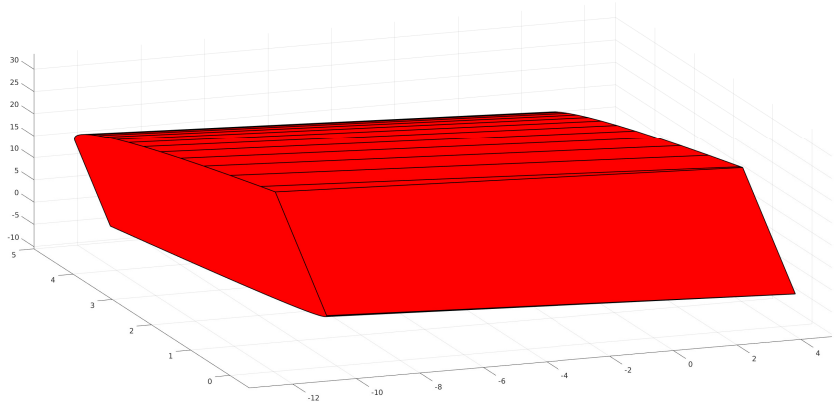

Figure 3: Invariant Set computed for scenario 1 by following an LQR Control Law

Solution 9: MPC controller 1: Closed Loop Simulations in Scenario 1 *(5 pts.)*

The plots in Figures 4 and 5 show the closed-loop simulation of scenario 1, obtained by following a receding horizon model predictive control law with $N = 30$ and conditions as mentioned in the question, with initial temperatures $T_0^{(1)} = T_{sp} + [3, 1, 0]^T$ and $T_0^{(2)} = T_{sp} + [-1, -0.1, -4.5]^T$ respectively.

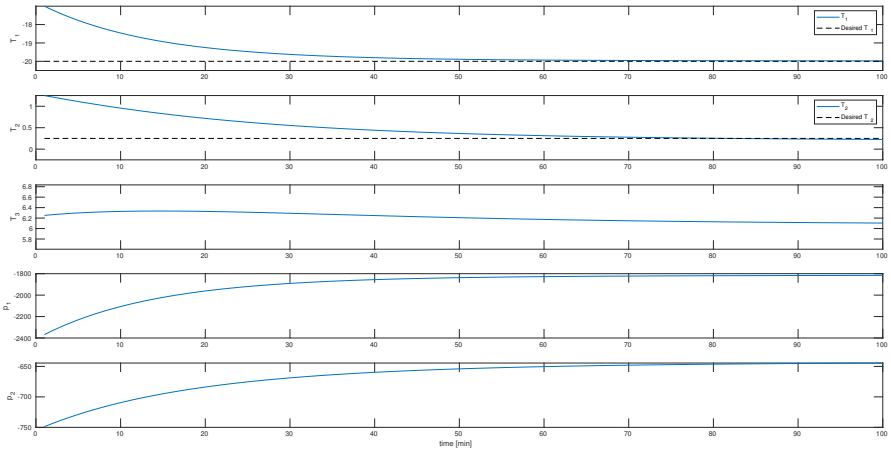

Figure 4: Closed-loop simulation of scenario 1 by following an MPC1 Control Law with initial setting $T_0^{(1)}$

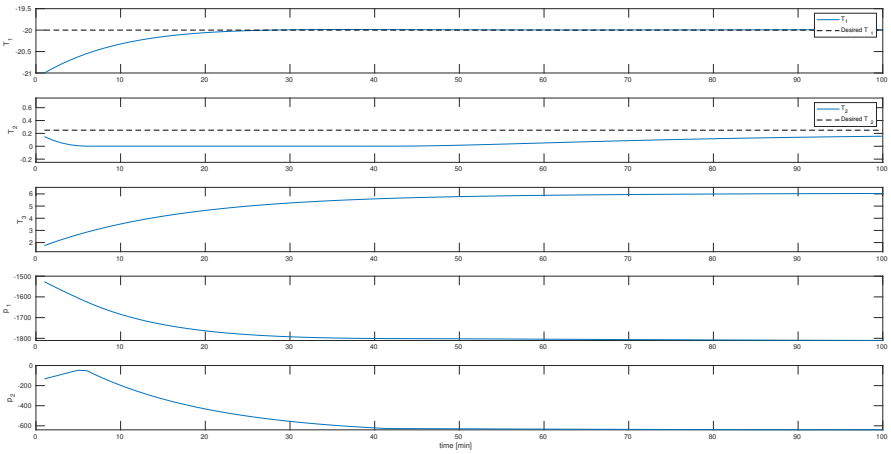

Figure 5: Closed-loop simulation of scenario 1 by following an MPC1 Control Law with initial setting $T_0^{(2)}$

Unlike the LQR controller from previous question, the model predictive controller *MPC 1* is able to drive the system to the desired equilibrium point T_{sp} without violating any constraints for either of the initial conditions.

The LQR controller does not violate the constraints in the case of $T_0^{(1)}$. However, for $T_0^{(2)}$, it does so. This can be explained through the invariant set. For the two given initial conditions: $T_0^{(1)} \in X_{LQR}$ while $T_0^{(2)} \notin X_{LQR}$. The LQR controller is an unconstrained controller and is only able to satisfy the constraints at all times when the initial state is inside the corresponding invariant set and the model is perfect.

Solution 10: Cost convergence in LQR and MPC 1 *(3 pts.)*

To show that the ∞-horizon cost for the LQR and MPC1 controllers are the same, we analyze both costs separately:

$$J^{\infty}_{LQR}(\mathbf{x}(0)) = \sum_{k=0}^{\infty} x_{LQR}(k)^T Q x_{LQR}(k) + u_{LQR}(k)^T R u_{LQR}(k)$$
$$J^{\infty}_{MPC}(\mathbf{x}(0)) = \sum_{k=0}^{\infty} x_{MPC}(k)^T Q x_{MPC}(k) + u_{MPC}(k)^T R u_{MPC}(k)$$

If the initial state $x(0)$ is the same for both of the controllers and it is inside the control invariant set X_{LQR}, the state trajectory obtained by executing either of the controllers would remain inside the invariant set at all times and the constraints would not be violated.

Since both the controllers optimize over the same cost and initial state (which lies in the invariant set) is the same, the optimal input computed at every time step would be the same, i.e.

$$u^*_{LQR}(k) = u^*_{MPC}(k); \forall k \in \{0, 1, 2, ...N\}$$

This would make the state evolves in the same way for both controllers (since the system dynamics are the same) $\implies x_{LQR}(k) = x_{MPC}(k); \forall k \in \{0, 1, 2, ...N\}$.

Using above reasoning and given that cost matrices Q and R are equal for the two controller's optimization problem, we can conclude that:

$$J^{\infty}_{LQR}(\mathbf{x}(0)) = J^{\infty}_{MPC1}(\mathbf{x}(0))$$

Solution 11: MPC controller 2: Asymptotically stable equilibrium point *(2 pts.)*

A closed-loop system is guaranteed to be asymptotically stable if its optimal cost function is a Lyapunov function. To show that the cost is a Lyapunov function, it is equivalent to proving that: $J^*(x(k+1)) < J^*(x(k))$.

Since we have the constraint that $x_N = 0$, we have a zero terminal cost i.e. $l_f(x_N) = 0$.

Suppose we start at $x(k)$ with the MPC solution $\mathcal{U}^* = \{u_0^*, u_1^*, ..., u_{N-1}^*\}$ which results in $\tilde{\mathcal{X}} = \{x_0^* = x(k), ..., \underbrace{x_N^* = 0}_{\text{termination}}\}$. Applying the control input $u(k) = u_0^*$, the N-stages cost-to-go for the optimal controller is given by:

$$J^*(x(k)) = \sum_{i=0}^{N-1} l(x_i^*, u_i^*) + l_f(\underbrace{x_N^*}_{=0}) = \sum_{i=0}^{N-1} l(x_i^*, u_i^*) + l_f(0)$$

We construct a candidate solution such that $\tilde{\mathcal{U}}^* = \{u_1^*, u_2^*, ..., u_{N-1}^*, 0\}$ which results in $\tilde{\mathcal{X}} = \{x_1^* = x(k+1), ..., x_N^* = 0, \underbrace{x_{N+1}^* = 0}_{A.0+B.0}\}$. Although $\tilde{\mathcal{U}}$ is not optimal, it is feasible as $\tilde{\mathcal{U}} \subset \mathcal{U}$. The N-stages cost-to-go for this candidiate solution would be:

$$\begin{aligned}\tilde{J}(x(k+1)) &= \sum_{i=1}^{N} l(x_i^*, u_i^*) + l_f(\underbrace{x_{N+1}^*}_{=0}) \\ &= \sum_{i=1}^{N-1} l(x_i^*, u_i^*) + l(x_N^*, 0) + l_f(0)\end{aligned}$$

Using above and the optimality assumption, we can write:

$$\begin{aligned}J^*(x(k+1)) - J^*(x(k)) \leq& \tilde{J}(x(k+1)) - J^*(x(k)) \\ &= -l(x_0^*, u_0^*) \\ &= -\underbrace{l(x(k), u(k))}_{\succ 0}\end{aligned}$$

This satisfies the Lyapunov decrease criterio implying that the cost function is indeed a Lyapunov function. Thus, the equilibrium point is asymptotically stable for the feasible set.

Solution 12: MPC controller 2: Closed Loop Simulation for $T_0^{(1)}$ *(3 pts.)*

The plot in Figure 6 shows the closed-loop simulation of scenario 1, with initial temperatures $T_0^{(1)} = T_{sp} + [3, 1, 0]^T$, obtained by following a receding horizon model predictive control law with $N = 30$ and conditions as mentioned in the question.

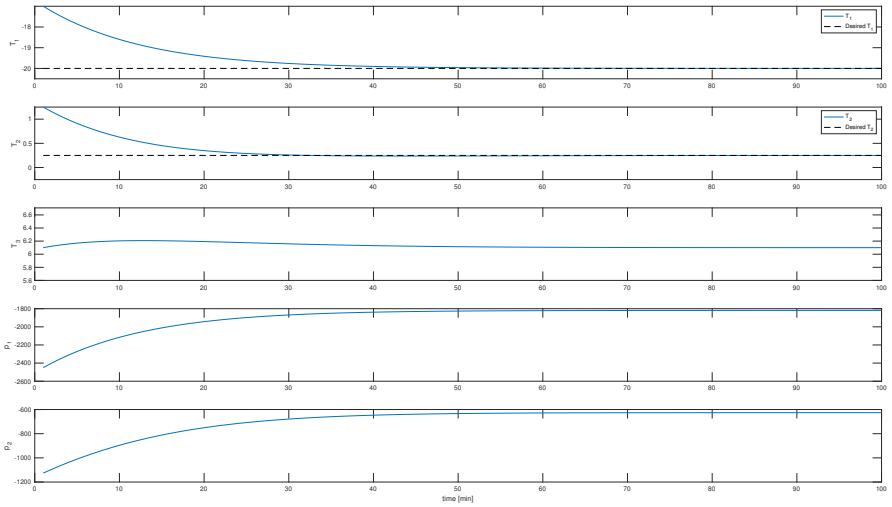

Figure 6: Closed-loop simulation of scenario 1 by following an MPC2 Control Law with initial setting $T_0^{(1)}$

Solution 13: Cost comparison between MPC controllers 1 and 2 *(2 pts.)*

Table 1 provides the cost for the MPC controllers with a horizon of $N = 30$.

Initial Temp.	**MPC 1**	**MPC 2**
$T_0^{(1)}$	336526.22	509342.65
$T_0^{(2)}$	249887.00	NaN

Table 1: Controller cost for MPC 1 and 2 for different initial settings

Providing the hard constraint for $\mathbf{x}_{30} = 0$, in MPC 2 leads to more aggressive input actions as the system tries to satisfy this constraint. Thus, for the initial state $T_0^{(1)}$, the cost for the MPC 2 is more than that for MPC1.

Further, MPC 2 is in-feasible with initial condition $T_0^{(2)}$. This is so because with the terminal state constraint $x_{30} = 0$ the feasibility set for the controller shrinks making the initial state $T_0^{(2)}$ lie outside this set.

Solution 14: MPC controller 3: Choosing the terminal cost *(2 pts.)*

We choose the terminal cost to be $X_N^T P_\infty X_N$ where P_∞ is the solution to the discrete-time algebraic Riccati equation:

$$P_\infty = A^T P_\infty A + Q - A^T P_\infty B(B^T P_\infty A)$$

As presented in Lecture 6 (Slide 48), the chosen terminal cost is a continuous Lyapunov function in the terminal set X_f and satisfies:

$$\begin{aligned}
&X_{k+1}^T P_\infty X_{k+1} - X_k^T P_\infty X_k \\
&= X_k^T(-P_\infty + A^T P_\infty A + F_\infty^T B^T P_\infty A - F_\infty^T R F_\infty) X_k \\
&= X_k^T(-P_\infty) + A^T P_\infty A - A^T P_\infty B(B^T P_\infty B + R)^{-1} B^T P_\infty A - F_\infty^T R F_\infty) X_k \\
&= -X_k^T (Q + F_\infty^T R F_\infty)_{\succ 0} X_k
\end{aligned}$$

With this we show that the origin is an asymptotically stable equilibrium point for the resulting closed-loop system.

Solution 15: MPC controller 3: Closed Loop Simulations in Scenario 1 *(3 pts.)*

The plots in Figures 7 and 8 show the closed-loop simulation of scenario 1 obtained by following a receding horizon model predictive control law with $N = 30$ and conditions as mentioned in the question with initial temperatures $T_0^{(1)} = T_{sp} + [3, 1, 0]^T$ and $T_0^{(2)} = T_{sp} + [-1, -0.1, -4.5]^T$ respectively.

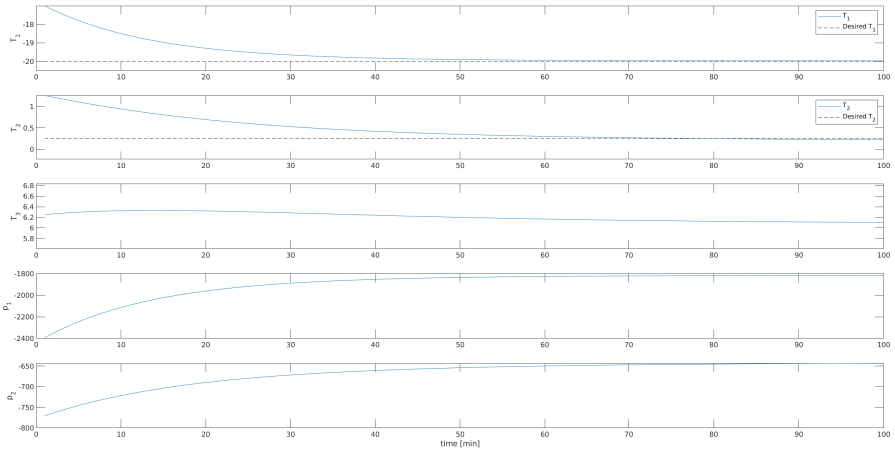

Figure 7: Closed-loop simulation of scenario 1 by following an MPC3 Control Law with initial setting $T_0^{(1)}$

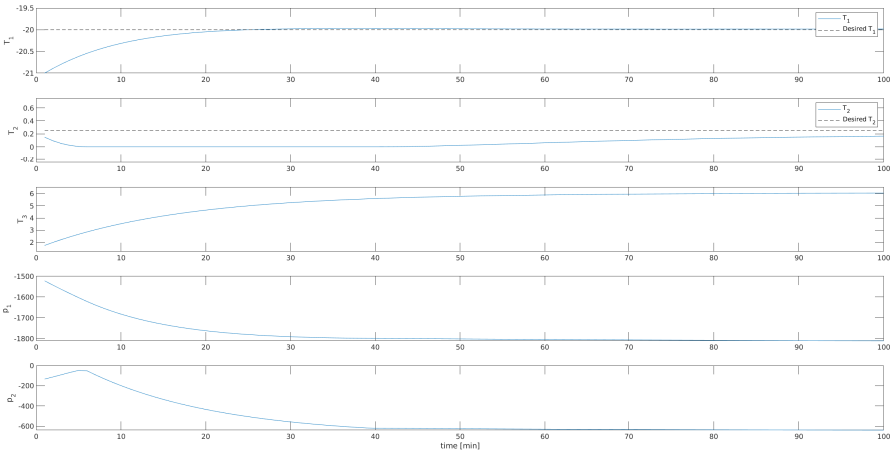

Figure 8: Closed-loop simulation of scenario 1 by following an MPC3 Control Law with initial setting $T_0^{(2)}$

Comparing the results obtained from MPC controller 3 and MPC controller 1, we find that the resulting trajectories are similar for both the initial conditions $T_0^{(1)}$ and $T_0^{(2)}$. Inspecting the two MPC formulations, the only difference is with the additional constraint on the terminal state of the receding horizon problem, $x_N \in \mathcal{X}_{LQR}$ for the MPC controller 3. However, as the two initial temperatures still lie in the feasibility set for both the controllers, the controllers would act similar and thereby the state trajectories observed would be similar.

Solution 16: Feasibility comparison for $T_0^{(2)}$ with MPC3 and MPC2 *(2 pts.)*

The initial condition $T(0) = T_0^{(2)}$ lies outside the feasibility set for MPC2 since we enforce a point terminal constraint of $X_{30} = 0$. However, by relaxing this constraint and allowing the terminal state $X_{30} \in \mathcal{X}_{LQR}$, which contains the point $X_{30} = 0$, we enlarge the region of attraction for the MPC3 controller compared to that for MPC2 controller. The new enlarged feasibility set for MPC3 includes the initial condition $T(0) = T_0^{(2)}$, thereby providing a trajectory that does not violate the specified constraints at all times and reaches the steady state.

Solution 17: MPC controller 3: Closed Loop Simulations in Scenario 2 *(2 pts.)*

The plot in Figure 9 shows the closed-loop simulation obtained by using model predictive control law with initial conditions: $T_0^{(2)}$ for scenario 2.

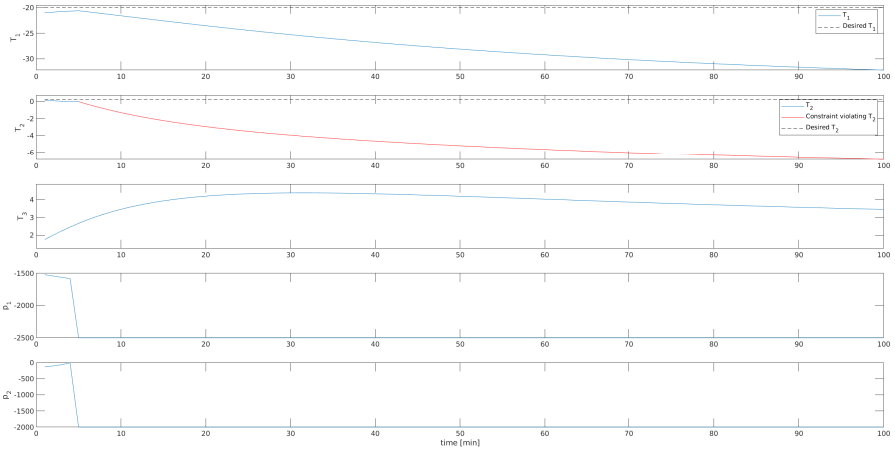

Figure 9: Closed-loop simulation of scenario 2 by following an MPC3 Control Law with initial setting $T_0^{(2)}$

Unlike in scenario 1 where the disturbances are zero in magnitude, for all timesteps, scenario 2 contains an initial disturbace which is quite high in magnitude. The MPC controller 3 violates the constraints for initial condition $T = T_0^{(2)}$ under scenario 2 since under the delta formulation, the assumption that the disturbances are constant is no longer valid. This shows that MPC controller 3 is not robust to error in the modelling of the system or while accounting the disturbances. Further, we also notice that once the state goes outside the region of attraction, it is not able to come back to it even though the unmodeled disturbances become zero.

Solution 18: MPC controller 4: Closed Loop Simulations in Scenario 2 *(4 pts.)*

The plot in Figure 10 shows the closed-loop simulation obtained by using model predictive control law with initial conditions: $T_0^{(2)}$ for scenario 2.

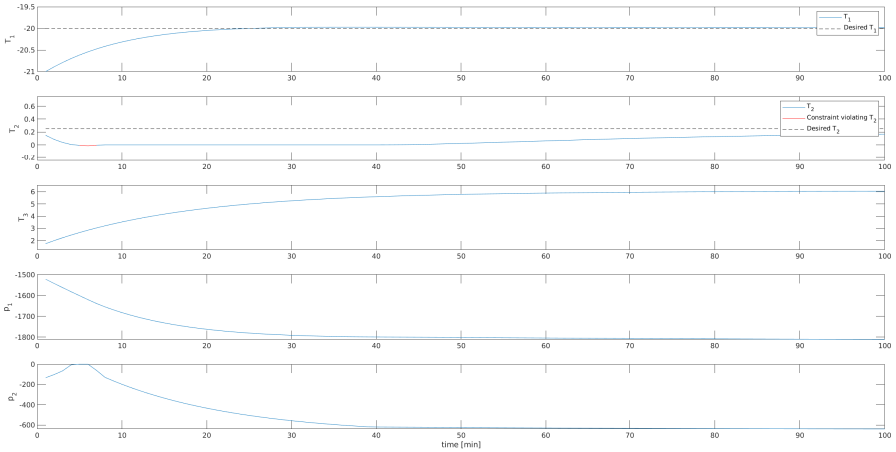

Figure 10: Closed-loop simulation of scenario 2 by following an MPC4 Control Law with initial setting $T_0^{(2)}$

Solution 19: MPC controllers 3 and 4: Closed Loop Simulations in Scenario 1 *(2 pts.)*

The plot in Figures 11 and 12 shows the closed-loop simulation obtained by using model predictive control laws 3 and 4 respectively, with initial conditions: $T_0^{(2)}$ for scenario 1.

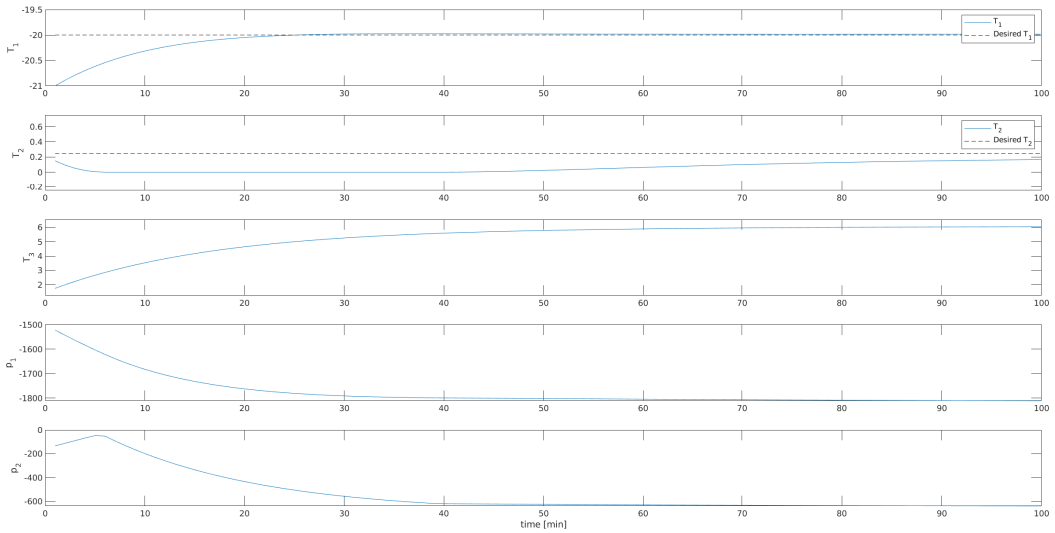

Figure 11: Closed-loop simulation of scenario 1 by following an MPC3 Control Law with initial setting $T_0^{(2)}$

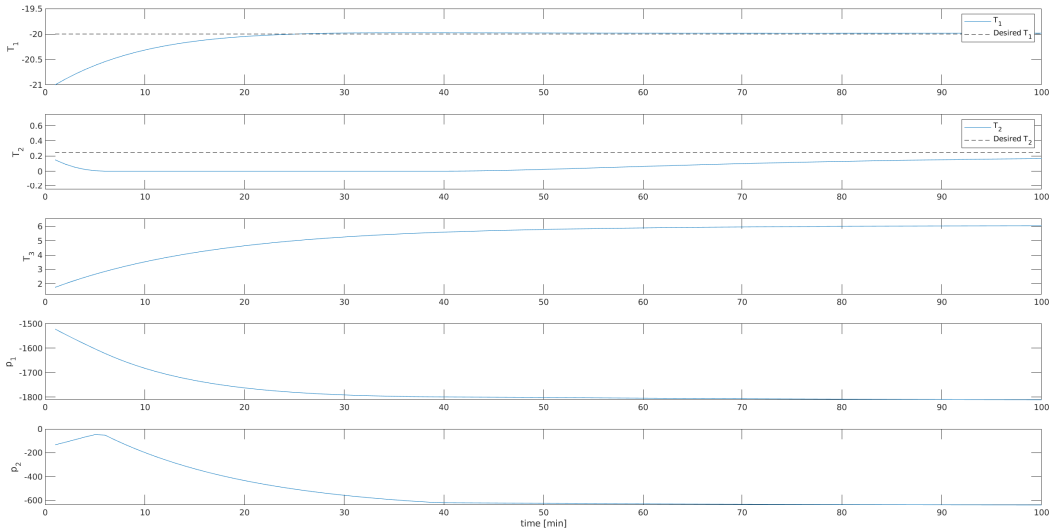

Figure 12: Closed-loop simulation of scenario 1 by following an MPC4 Control Law with initial setting $T_0^{(2)}$

Solution 20: MPC controllers 5: Augmenting the discrete-time system *(2 pts.)*

To account for the time-varying disturbance, we augment the disturbance d into our state representation $z = [x, d]^T$. The disturbance is modelled through an integral disturbance dynamics.

$$\begin{pmatrix} x(k+1) \\ d(k+1) \end{pmatrix} = A_{aug} \begin{pmatrix} x(k) \\ d(k) \end{pmatrix} + B_{aug} u(k)$$
$$y(k) = C_{aug} \begin{pmatrix} x(k) \\ d(k) \end{pmatrix} + D_{aug} u(k)$$

where:

$$A_{aug} = \begin{pmatrix} A & B_d \\ 0 & I \end{pmatrix} = \begin{pmatrix} 0.9749 & 0.0216 & 0.0003 & 0.0003 & 0.0000 & 0.0000 \\ 0.0108 & 0.9458 & 0.0283 & 0.0000 & 0.0001 & 0.0000 \\ 0.0001 & 0.0226 & 0.9421 & 0.0000 & 0.0000 & 0.0001 \\ 0 & 0 & 0 & 1.0000 & 0 & 0 \\ 0 & 0 & 0 & 0 & 1.0000 & 0 \\ 0 & 0 & 0 & 0 & 0 & 1.000 \end{pmatrix}$$

$$B_{aug} = \begin{pmatrix} B \\ 0 \end{pmatrix} = 10^{-3} * \begin{pmatrix} 0.2962 & 0.0016 \\ 0.0016 & 0.1459 \\ 0.0000 & 0.0017 \\ 0 & 0 \\ 0 & 0 \\ 0 & 0 \end{pmatrix}$$

$$C_{aug} = \begin{pmatrix} C & 0 \end{pmatrix} = \begin{pmatrix} I & 0 \end{pmatrix}$$

$$D_{aug} = \begin{pmatrix} 0 \\ 0 \end{pmatrix}$$

For the new system $(A_{aug}, B_{aug}, C_{aug}, D_{aug})$, we confirm that the augmented system is observable by checking that (A, C) is observable and the matrix: $\begin{bmatrix} A - \mathbb{I} & B_d \\ C & C_d \end{bmatrix}$ has full column rank (i.e: rank $= n_x + n_d = 6$)

Solution 21: MPC controllers 5: Design the observer gain matrix L *(2 pts.)*

Similar to the way we proceeded in Solution 3, we compute the steady state based on the estimated disturbances using the following expression: $M = \begin{bmatrix} \mathbb{I} - A & B \\ H & 0 \end{bmatrix}$, where $H = \begin{bmatrix} 1 & 0 & 0 \\ 0 & 1 & 0 \end{bmatrix}$ is the selection matrix, and $\mathbf{r}$ is the reference state.

The steady state needs to be computed at every timestep to account for the new estimated disturbance. This evaluation is done by solving the the following expression:

$$\begin{bmatrix} \mathbf{X}_{sp} \\ \mathbf{p}_{sp} \end{bmatrix} = M^{-} \begin{bmatrix} B_d \hat{\mathbf{d}} \\ \mathbf{r} \end{bmatrix}$$

Using the formulation as presented in the question, the state observer for the augmented model can be written as:

$$\begin{pmatrix} x(k+1) \\ d(k+1) \end{pmatrix} = A_{aug} \begin{pmatrix} x(k) \\ d(k) \end{pmatrix} + B_{aug} u(k) + L \left(y(k) - C_{aug} \begin{pmatrix} x(k) \\ d(k)) \end{pmatrix} \right)$$

The error dynamics for the estimator is shown below where $\hat{x}$ and $\hat{d}$ are estimates of the state and disturbances on the system respectively.

$$\begin{aligned} \begin{pmatrix} x(k+1) - \hat{x}(k+1) \\ d(k+1) - \hat{d}(k+1) \end{pmatrix} &= \begin{pmatrix} A & B_d \\ 0 & I \end{pmatrix} \begin{pmatrix} x(k) - \hat{x}(k) \\ d(k) - \hat{d}(k) \end{pmatrix} - \begin{pmatrix} L_x \\ L_d \end{pmatrix} \Big(C\hat{x}(k) + C_d \hat{d}(k) - Cx(k) - C_d d(k) \Big) \\ &= (A_{aug} + L C_{aug}) \begin{pmatrix} x(k) - \hat{x}(k) \\ d(k) - \hat{d}(k) \end{pmatrix} \end{aligned}$$

We choose observer gain matrix $L = [L_x, L_d]^T$ by placing the poles such that the error dynamics is stable and converges to zero (i.e the estimator is asymptotically stable).

The resulting eigen values for the error dynamics system are: $\lambda = 0, 0, 0, 0.05, 0.05, 0.05()$.

Solution 22: MPC controllers 5: Deriving the offset-free MPC formulation *(6 pts.)*

The plot in Figures 13 shows the closed-loop simulation of MPC controller 3 in scenario 3, with initial temperatures $T_0^{(1)} = T_{sp} + [3, 1, 0]^T$. Figure 14 shows the closed-loop simulation of MPC controller 5 in scenario 3, with initial temperatures $T_0^{(1)} = T_{sp} + [3, 1, 0]^T$.

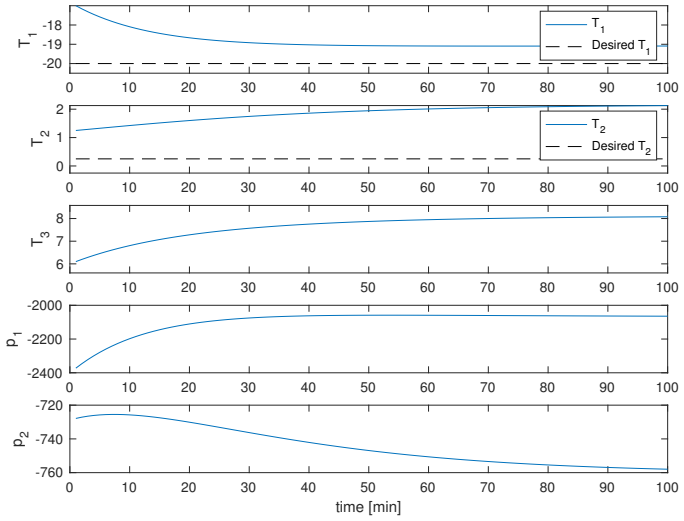

Figure 13: Closed-loop simulation of scenario 3 by following an MPC3 Control Law with initial setting $T_0^{(1)}$

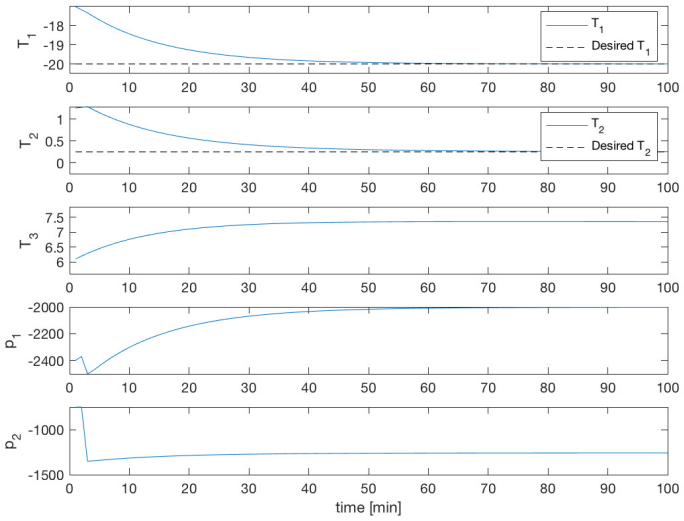

Figure 14: Closed-loop simulation of scenario 3 by following an MPC5 Control Law with initial setting $T_0^{(1)}$

The MPC controller 3 shows an offset in case of unknown model errors (or disturbances) since it does not account for them (similar to the case in scenario 2). However, by augmenting the distrubances into the state and using the augmented model to estimate the temperatures and disturbance, the offset is removed as we see for the case of MPC controller 5. We also have to modify the system's steady state at each timestep to account for effect of disturbance. This modifies the target to account for effect of disturbance on tracked variables.

Solution 23: MPC controller 1: Implementation using FORCES Pro *(3 pts.)*

To compare the efficiency of YALMIP optimizer (used in controller MPC1) and the FORCES optimizer, the runtime for solving the optimization problem is computed (without considering the time to initialize the solver). The statistics over the observed runtime for the two implementations of MPC 1 in a set of 10 runs is shown in Table 2.

Implementation	**Mean (in sec)**	**Std. Dev. (in sec)**
YALMIP	0.8853	0.1371
Forces PRO	0.1009	0.0112

Table 2: Statistics over 10 runs for two implementations of MPC 1 Controller

It can be seen FORCES Pro implementation ~ 8.75 times faster than the YALMIP based solver. This is expected as FORCES Pro generates a C++ mex file which is supposed to have lower execution time.